# Evidence for strong correlations at finite temperatures in the dimerized magnet $Na_2Cu_2TeO_6$

Yanyan Shangguan,[1,*] Song Bao,[1,*] Zhao-Yang Dong,[2,*] Zhengwei Cai,[1] Wei Wang,[3] Zhentao Huang,[1] Zhen Ma,[4] Junbo Liao,[1] Xiaoxue Zhao,[1] Ryoichi Kajimoto,[5] Kazuki Iida,[6] David Voneshen,[7,8] Shun-Li Yu,[1,9,†] Jian-Xin Li,[1,9,‡] and Jinsheng Wen[1,9,§]

[1]*National Laboratory of Solid State Microstructures and Department of Physics, Nanjing University, Nanjing 210093, China*
[2]*Department of Applied Physics, Nanjing University of Science and Technology, Nanjing 210094, China*
[3]*School of Science, Nanjing University of Posts and Telecommunications (NUPT), Nanjing 210023, China*
[4]*Institute for Advanced Materials, Hubei Normal University, Huangshi 435002, China*
[5]*J-PARC Center, Japan Atomic Energy Agency (JAEA), Tokai, Ibaraki 319-1195, Japan*
[6]*Neutron Science and Technology Center, Comprehensive Research Organization for Science and Society (CROSS), Tokai, Ibaraki 319-1106, Japan*
[7]*ISIS Facility, Rutherford Appleton Laboratory, Chilton, Didcot, Oxon OX11 0QX, United Kingdom*
[8]*Department of Physics, Royal Holloway University of London, Egham TW20 0EX, United Kingdom*
[9]*Collaborative Innovation Center of Advanced Microstructures, Nanjing University, Nanjing 210093, China*

(Received 30 September 2021; revised 30 November 2021; accepted 20 December 2021; published 27 December 2021)

Dimerized magnets forming alternating Heisenberg chains exhibit quantum coherence and entanglement and thus can find potential applications in quantum information and computation. However, magnetic systems typically undergo thermal decoherence at finite temperatures. Here, we show inelastic neutron scattering results on an alternating antiferromagnetic-ferromagnetic chain compound $Na_2Cu_2TeO_6$ that the excited quasiparticles can counter thermal decoherence and maintain strong correlations at elevated temperatures. At low temperatures, we observe clear dispersive singlet-triplet excitations arising from the dimers formed along the crystalline *b* axis. The excitation gap is of ∼18 meV and the bandwidth is about half of the gap. The band top energy has a weak modulation along the [100] direction, indicative of a small interchain coupling. The gap increases while the bandwidth decreases with increasing temperature, leading to a strong reduction in the available phase space for the triplons. As a result, the Lorentzian-type energy broadening becomes highly asymmetric as the temperature is raised. These results are associated with a strongly correlated state resulting from hard-core constraint and quasiparticle interactions. We consider these results to be not only evidence for strong correlations at finite temperatures in $Na_2Cu_2TeO_6$, but also for the universality of the strongly correlated state in a broad range of quantum magnetic systems.

DOI: 10.1103/PhysRevB.104.224430

## I. INTRODUCTION

Spin-chain systems confined to one dimension provide an excellent simple platform in studying the quantum magnetism [1]. In particular, spin-chain compounds with Heisenberg interactions alternating between the intradimers and interdimers have been studied extensively by means of inelastic neutron scattering (INS) [2–14]. These materials have an $S = 0$ singlet ground state, in which two neighboring antiparallel spins within a dimer bind together to form a quantum mechanical singlet, and effectively the system does not exhibit long-range order even down to zero temperature. The spectra feature a singlet-triplet excitation separated by a gap $\Delta$, the energy required to flip a spin within a singlet. The triplet excitations correspond to the triply degenerate spin $S = 1$ quasiparticles termed triplons, which may exhibit topological properties due to the presence of Dzyaloshinskii-Moriya interactions or competing exchange couplings [15–21]. The Hamiltonian for an alternating Heisenberg chain system can be written as [14,22,23]

$$H = \sum_{i=1,N/2} J_1 \boldsymbol{S}_{2i-1} \cdot \boldsymbol{S}_{2i} + J_2 \boldsymbol{S}_{2i} \cdot \boldsymbol{S}_{2i+1}, \tag{1}$$

where $N$ is the total number of spins in a chain, $J_1$ and $J_2$ are the interactions for the spins within a dimer and between the nearest-neighbor dimers, respectively, and $\eta = |J_2/J_1|$, which is typically less than 1 is the alternating parameter. A finite $J_2$ will give rise to the dispersive excitation spectra. To the lowest order of the interdimer interactions, the dispersion can be simplified as [14,22,23]

$$E(\boldsymbol{Q}) = J_1 - \frac{J_2}{2}\cos(\boldsymbol{Q}d), \tag{2}$$

where $\boldsymbol{Q}$ is the wave vector and $d$ is the distance between the nearest-neighbor dimers (from center to center). In this case, $\Delta$ and the bandwidth $B$ can be approximated to be

*These authors contributed equally to this work.
†slyu@nju.edu.cn
‡jxli@nju.edu.cn
§jwen@nju.edu.cn

 

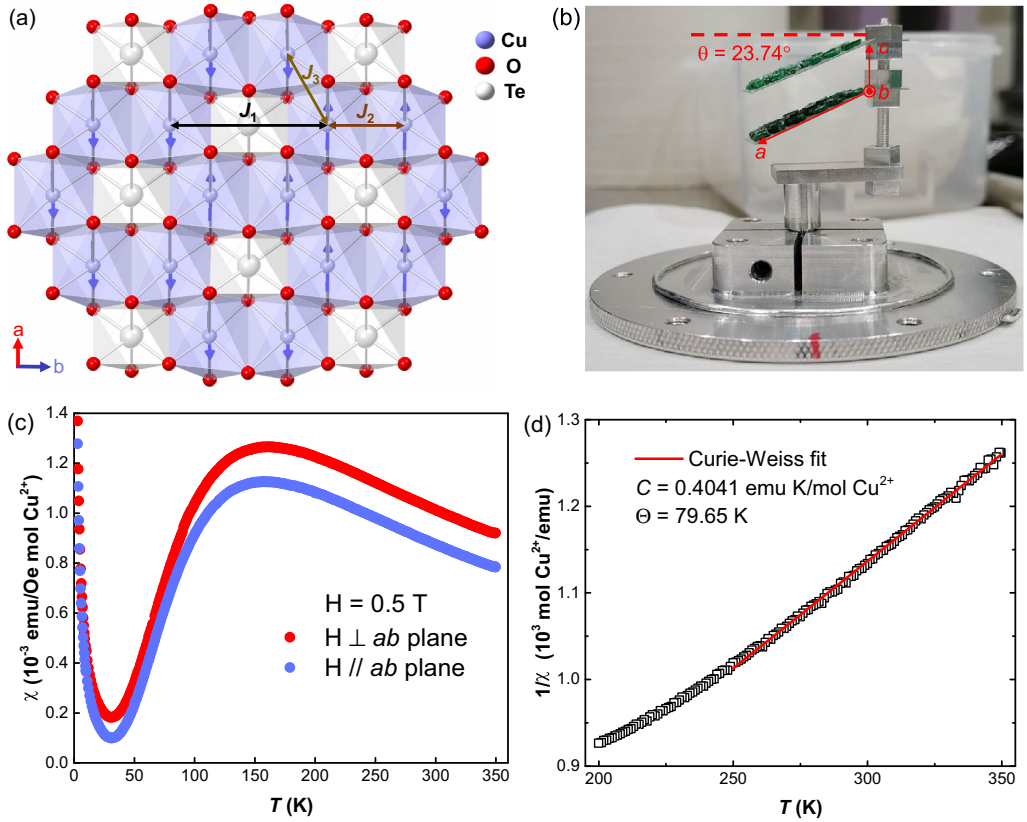


FIG. 1. (a) Schematic $Cu_2TeO_6$ layer structure of $Na_2Cu_2TeO_6$. Arrows denote the spins. $J_1$, $J_2$, and $J_3$ represent the intradimer (antiferromagnetic), interdimer (ferromagnetic), and interchain (ferromagnetic) couplings, respectively. (b) Coaligned single crystals we used for the INS measurements. This photo only shows 60 pieces of single crystals, whereas in the actual measurements we used 90 pieces glued on 3 aluminum plates. The aluminum plates were well tilted by 23.74° so that the horizontal plane was the ($H$, $K$, 0) plane. (c) Temperature dependence of the magnetic susceptibility measured with magnetic field of $\mu_0 H = 0.5$ T applied parallel and perpendicular to the $a$-$b$ plane. There is some anisotropy of the spin susceptibility, which may be due to the quasi-one-dimensional magnetic structure and impurity spins. (d) Inverse magnetic susceptibility of $Na_2Cu_2TeO_6$ between 200 and 350 K. The solid line represents a fit to the data with the Curie-Weiss law over the interval from 250 to 350 K, yielding the parameters indicated in the figure.

$J_1 - |J_2|/2$ and $|J_2|$, respectively. This indicates the critical role of $\eta$ in controlling the available phase space for the triplons.

Recently, a dimerized magnet $Na_2Cu_2TeO_6$ was proposed to be a quasi-one-dimensional chain system [24–30]. It has a monoclinic structure with the space group $C2/m$, and consists of alternating $Cu_2TeO_6$ magnetic layers and Na nonmagnetic layers stacking along the $c$ axis in a monoclinic way [24], similar to $Na_3Cu_2SbO_6$ (Refs. [31,32]). In the $Cu_2TeO_6$ layer, six $CuO_6$ octahedra form a distorted honeycomb lattice via edge-sharing with a $TeO_6$ octahedron at the center as shown in Fig. 1(a). Each $Cu^{2+}$ with spin-1/2 interacts with three neighboring spins [Fig. 1(a)], but it has been suggested that the third-neighbor interchain coupling ($J_3$) can be ignored and only the antiferromagnetic (AFM) $J_1$ and ferromagnetic (FM) $J_2$ along the $b$ axis dominate, making $Na_2Cu_2TeO_6$ a quasi-one-dimensional alternating AFM-FM system [24–28]. Interestingly, the magnitude of $J_1$ is larger than that of $J_2$ although it involves a super-superexchange path Cu-O-Te-O-Cu, which is much longer [24]. Very recently, Gao *et al.* have performed INS measurements on a single crystal of $Na_2Cu_2TeO_6$, which reveal clear singlet-triplet excitations [30]. In Ref. [30], they show the excitation spectra with a gap of ∼18 meV can be described by a Hamiltonian with $J_1 = 22.78(2)$ meV, $J_2 = -8.73(4)$ meV, and a small but non-negligible antiferromagnetic $J_3 = 1.34(3)$ meV. These results place $Na_2Cu_2TeO_6$ in a unique position [30]. First, the large gap and small bandwidth in $Na_2Cu_2TeO_6$ make the available phase space for the triplons severely limited. Second, the interactions alternate antiferromagnetically and ferromagnetically along the chain. Third, it has a small but finite interchain coupling, which preserves the weak two-dimensional nature of the magnetic interactions. One intriguing property of the dimerized magnets with limited phase space is that a strongly correlated state at high temperatures may be retained due to the hard-core constraint (only one quasiparticle is allowed per dimer even for bosons) and quasiparticle interactions [33–41]. The strong correlations at finite temperatures, which can be characterized by the asymmetric Lorentzian-type broadening of the energy scans instead of the symmetric Lorentzian-type broadening as in conventional magnets, have been observed in spin chains [37,40–43], spin ladders [44,45], and three-dimensional gapped quantum magnet $Sr_3Cr_2O_8$ (Refs. [38,39]), but not in two-dimensional AFM-FM alternating chain compounds yet. Considering these [24,30], $Na_2Cu_2TeO_6$ provides an ideal platform to investigate the

universality of the strongly correlated state at elevated temperatures in quantum magnets.

Here, we report comprehensive results of INS measurements on $Na_2Cu_2TeO_6$ and focus on the temperature dependence of the spectra. Our results reveal that $Na_2Cu_2TeO_6$ is an alternating AFM-FM chain compound with weak but non-negligible interchain coupling, in excellent agreement with a previous paper [30]. Interestingly, by following the temperature dependence of the excitation spectra, we find that the gap increases while the bandwidth decreases with increasing temperature, thus limiting the available phase space for the triplons. In the meantime, we observe an asymmetric Lorentzian-type energy broadening, which gets more pronounced as the temperature is raised. We attribute this to the thermally activated strongly correlated state arising from hard-core constraint and quasiparticles interactions. Our results on the asymmetric Lorentzian-type energy broadenings are compelling evidence for the strong correlations at finite temperatures in $Na_2Cu_2TeO_6$, and indicate the universal presence of strongly correlated state in a broad range of quantum systems.

## II. EXPERIMENTAL DETAILS

Polycrystalline powders of $Na_2Cu_2TeO_6$ were synthesized by a standard solid-state reaction method, and single crystals were successfully grown by the flux method as described in Ref. [29]. The grown translucent green crystals with *a*-*b* plane as the cleavage plane have a typical mass of 30 mg for each piece. Magnetic susceptibility measurements were conducted using the vibrating sample magnetometer option integrated in a Physical Property Measurement System (PPMS-9T) from Quantum Design.

For INS experiments, single crystals were glued onto aluminum plates by hydrogen-free Cytop grease. These crystals were well coaligned using a backscattering Laue x-ray diffractometer. Neutron scattering experiments were performed on time-of-flight spectrometers MERLIN at ISIS facility in the United Kingdom [46] and 4SEASONS at J-PARC center in Japan [47]. We coaligned 90 pieces of single crystals weighed about 3 g in total for the experiments on MERLIN and 4SEASONS. As shown in Fig. 1(b), single crystals were coaligned onto the rectangular aluminum plates with $a$ and $b$ axes oriented along the edge directions of the aluminum plate. These crystals were well aligned so that the overall mosaic spread was $\sim 0.3^\circ$ as determined from the rocking scan through the (2, 0, 0) peak. The aluminum plates were well tilted by $23.74^\circ$ so that the horizontal plane was the ($H$, $K$, 0) plane. The assembly with ($H$, $K$, 0) as the horizontal plane was mounted in a closed-cycle refrigerator for neutron experiments.

For the measurements on MERLIN, we set the angle of the neutron beam direction parallel to the $b$ axis to be zero. Data were collected at 5 and 18 K with $E_i = 40.49$ meV by rotating the sample about the vertical direction with a range of $120^\circ$ in a $2^\circ$ step. As for the measurements on 4SEASONS, we used a primary $E_i = 55$ meV and a chopper frequency of 350 Hz with an energy resolution of 2.65 meV at the elastic line. Measurements were performed at 5, 90, 150, and 200 K. We set the angle where the [100] direction was parallel to the incident beam direction to be $0^\circ$. Data were collected by rotating the sample about the vertical axis from $-30^\circ$ to $150^\circ$ in a $1^\circ$ step. We counted 15 minutes for each step. Raw data were reduced and analyzed using Horace [48]. The wave vector $\boldsymbol{Q}$ was expressed as ($H$, $K$, $L$) reciprocal lattice unit (rlu) of $(a^*, b^*, c^*) = (2\pi/a\cos\theta,\ 2\pi/b,\ 2\pi/c\cos\theta)$ with $a = 5.706$ Å, $b = 8.6375$ Å, $c = 5.938$ Å, and $\theta = 113.74^\circ - 90^\circ = 23.74^\circ$, representing the angle between $a(c)$ and $a^*(c^*)$.

## III. RESULTS

### A. Sample characterizations and magnetic excitation spectra

We measured the magnetic susceptibility of the $Na_2Cu_2TeO_6$ single crystals with a vibrating sample magnetometer, and the results are shown in Figs. 1(c) and 1(d). From Fig. 1(c), the magnetic susceptibility does not show any signature of long-range order. There is a broad hump with its maximum around 150 K, which indicates the gradual establishment of short-range singlets below this temperature, and thus the susceptibility decreases. The hump signifies the existence of a spin gap. By fitting the susceptibility with an alternating AFM-FM chain model [22,26–28,49,50], a gap of $\Delta \sim 254$ K was estimated for $Na_2Cu_2TeO_6$ (Refs. [24,31]). The upturn at low temperatures is probably due to the impurity spins, which together with the quasi-one-dimensional magnetic structure may cause the anisotropy of the susceptibility with field applied in and out of the plane. Examination of the high-temperature data of the inverse magnetic susceptibility [Fig. 1(d)] shows that $\chi$ follows the Curie-Weiss law, with $\chi = C/(T + \Theta)$, from 250 to 350 K. From the Curie-Weiss fit, we obtain the Curie constant, $C = 0.4041$ emu K/mol $Cu^{2+}$, which is consistent with a spin-only effective magnetic moment $\mu_{\text{eff}} = 1.80\ \mu_B/Cu^{2+}$ with $S = 1/2$. This leads to a Landé $g$ factor of 2.08 for this compound, which is within the reasonable range for $Cu^{2+}$. The Curie-Weiss temperature $\Theta$ is 79.65 K, with the positive sign indicative of the dominant antiferromagnetic correlation. These results are in excellent agreement with previous studies on this compound [24,26–28,31].

We have performed INS measurements on the $Na_2Cu_2TeO_6$ single crystals, and the singlet-triplet excitation spectra along the $H$, $K$, and $L$ directions at $T = 5$ K are plotted in Fig. 2. These magnetic excitation spectra share a close similarity with those presented in Ref. [30]. To quantify the magnetic correlations of $Na_2Cu_2TeO_6$ and compare the extracted exchange coupling parameters with those in the previous study [30], random phase approximation calculations of the magnetic excitation spectra were performed. We first extracted the experimental dispersions from modified Lorentzian fits to constant-$\boldsymbol{Q}$ scans at 145 points along five high-symmetry directions, which were then fitted by the same dispersion relation utilized in Ref. [30]. The fitted parameters resulting from our fits are $J_1 = 22.82(7)$ meV, $J_2 = -8.47(8)$ meV, and $J_3 = 1.37(6)$ meV, which are almost the same as those of Ref. [30]. The calculated dispersions using these parameters are plotted on top of the experimental data as solid curves in Fig. 2. The calculated dispersions are in excellent agreement with the experimental results. Our theoretical calculations confirm the weakly two-dimensional

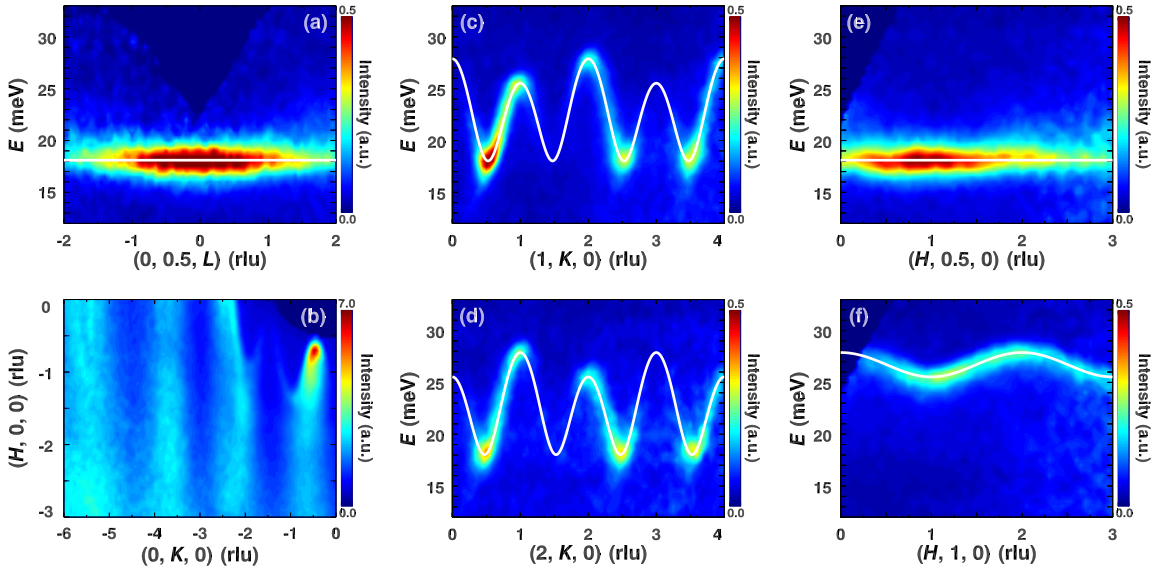


FIG. 2. Magnetic spectra of $Na_2Cu_2TeO_6$ measured at 5 K. (a) Scattering intensity measured along (0, 0.5, $L$) with integration widths of $\Delta H$ and $\Delta K$ of 0.2 rlu. (b) Contour map of the constant-energy cut measured with $E_i = 40.49$ meV, obtained on MERLIN at ISIS. The energy range of the integration is [15,30] meV. [(c)–(f)] INS spectra collected along (1, $K$, 0), (2, $K$, 0), ($H$, 0.5, 0), and ($H$, 1, 0) within the ($H$, $K$, 0) plane with $E_i = 55$ meV. The integration widths are $\Delta H = 0.2$ rlu, $\Delta K = 0.2$ rlu, and $\Delta L = 4$ rlu. Solid curves are the calculated dispersions using exchange parameters of $J_1 = 22.82(7)$ meV, $J_2 = -8.47(8)$ meV, and $J_3 = 1.37(6)$ meV. The data except (b) are from 4SEASONS at J-PARC.

nature of the magnetic interactions in $Na_2Cu_2TeO_6$, where the dimers are coupled to form alternating chains along the $b$ axis and the interchain coupling within the $a$-$b$ plane is weak but non-negligible [30]. Based on these magnetic excitation spectra, we explore their temperature evolution in details in the following.

### B. Strong correlated behaviors

The magnetic excitation spectra along (1.5, $K$, 0) at 5, 90, 150, and 200 K are plotted in Fig. 3. We can clearly observe the well-defined triplon excitations at low temperatures [Fig. 3(a)]. At 90 K, which is below the hump temperature, the triplon bands are still clearly resolvable, although the intensity becomes much weaker compared to that at 5 K. At 150 and 200 K, the excitations are much broader, but the excitations around $K = 0.5$, 2.5, and 3.5 rlu can still be identified. To further quantify the triplon band, we plot constant-$\boldsymbol{Q}$ scans at the band bottom (1.5, 0.5, 0) and band top (1.5, 1, 0) at different temperatures in Figs. 4(a)–4(d). As the temperature is raised, the scattering intensity gets weaker, and the peak width, especially for that at (1.5, 1, 0), becomes much larger. The temperature-induced intensity weakening and peak broadening are expected for a magnetic system. From Figs. 4(a)–4(d), we can extract the spin gap $\Delta$, bandwidth $B$, and the ratio of spin gap to bandwidth $\Delta/B$ at different temperatures. We take the peak center of the band bottom to be $\Delta$, and the energy interval between the centers of the band bottom and top to be $B$ as we illustrate by the shades in Figs. 4(a)–4(d).

These results are plotted in Figs. 4(e)–4(g). In Fig. 4(e), the gap increases monotonically with increasing temperature at $\boldsymbol{Q} = (1.5, 0.5, 0)$ obtained on 4SEASONS. This behavior is different from that of a magnetically ordered system where the gap size decreases with increasing temperature due to the reduced ordered magnetic moment. On the other hand, it is similar to the Haldane-chain compounds with integer spins, where the gap increases with temperature as a result of the reduced coherent length and finite-size effect [51,52]. The bandwidth, as presented in Fig. 4(f), decreases monotonically with temperature. This can also be visualized from

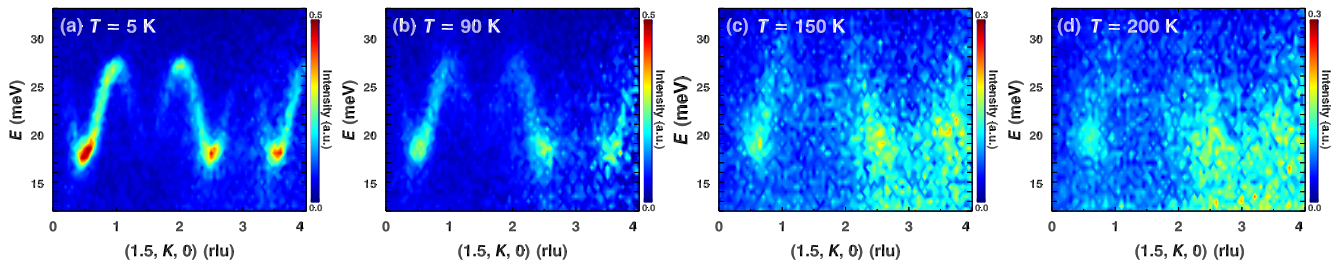


FIG. 3. Temperature dependence of the magnetic excitation spectra. [(a)–(d)] INS spectra along (1.5, $K$, 0) at $T = 5$, 90, 150, and 200 K, respectively, collected on 4SEASONS at J-PARC. The integration widths are $\Delta H = 0.2$ rlu, and $\Delta L = 4$ rlu.

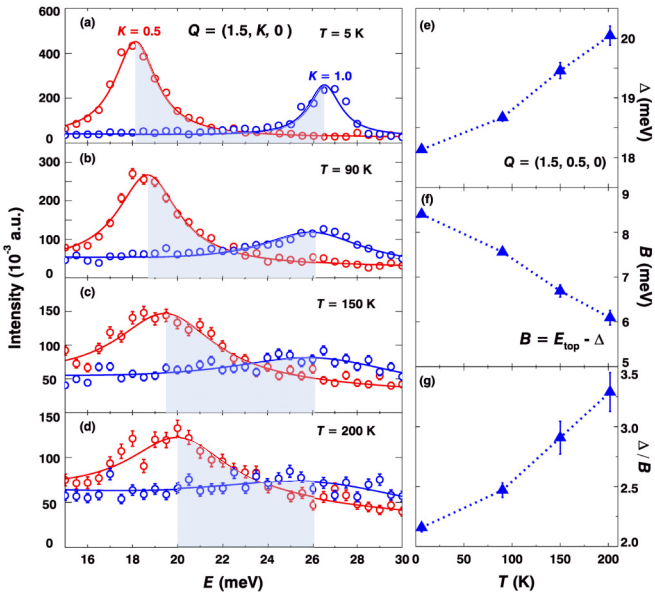


FIG. 4. [(a)–(d)] Constant-$\boldsymbol{Q}$ cuts upon the spectra of Fig. 3 at the band bottom (1.5, 0.5, 0) and band top (1.5, 1.0, 0) at 5, 90, 150, and 200 K, respectively. The integration intervals for $H$ and $K$ are both $\pm 0.1$ rlu, while for $L$ it is $\pm 2$ rlu. Solid lines correspond to the fits using Lorentzian function from which we extract the peak positions. The shades denote the bandwidth $B$, which is the energy interval between the centers of the band bottom and top. [(e)–(g)] Temperature dependence of gap energy $\Delta$, bandwidth $B$ and the ratio of spin gap to bandwidth $\Delta/B$, respectively.

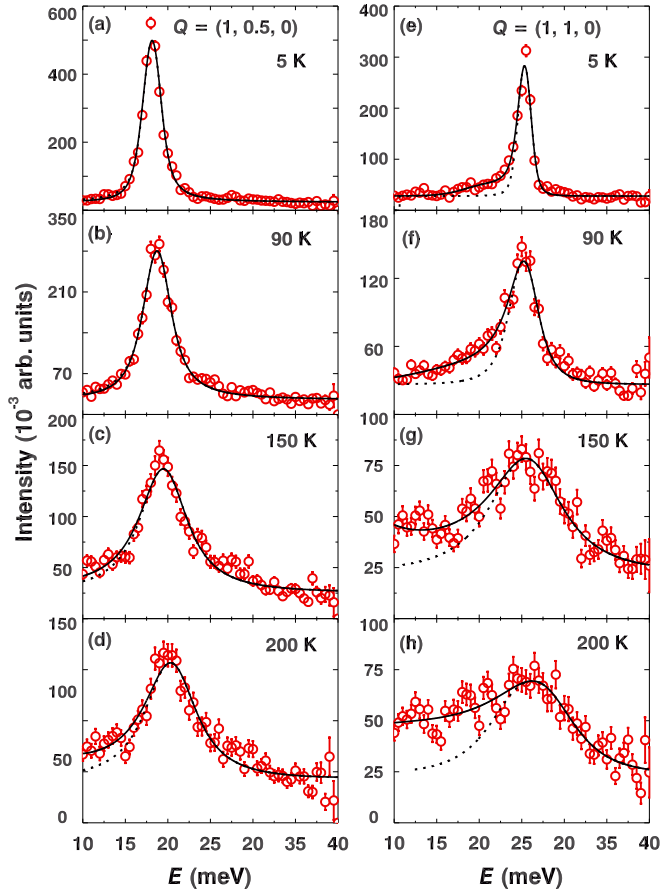


FIG. 5. [(a)–(d)] Constant-$\boldsymbol{Q}$ cuts at the band bottom (1, 0.5, 0), and [(e)–(h)] at the band top (1, 1, 0) at 5, 90, 150, and 200 K, obtained on 4SEASONS at J-PARC. The integration intervals for $H$ and $K$ are both $\pm 0.1$ rlu, while for $L$ it is $\pm 2$ rlu. Black solid lines correspond to the fits using Eq. (3). Dashed curves represent the symmetric Lorentzian fits.

Figs. 4(a)–4(d) by the shades, where the band bottom increases while the band top decreases from 5 to 200 K. As a consequence, the ratio of the gap to the bandwidth increases from 2.16 at 5 K to 3.29 at 200 K, as shown in Fig. 4(g). This ratio quantifies the available phase space for the triplons. A larger ratio results in a more limited available phase space, and hence the triplons will be localized and interacting strongly with each other. This is verified by analyzing the line shape of the constant-$\boldsymbol{Q}$ cuts at (1, 0.5, 0) and (1, 1, 0) at different temperatures in Fig. 5.

From Fig. 5, it is clear that the line shapes of the excitations do not simply broaden symmetrically with increasing temperature. At (1, 0.5, 0) at 5 K, the energy scan at the band bottom is sharp and symmetric [Fig. 5(a)]. As the temperature is increased, the peak becomes asymmetric with the tail extending towards lower energies. At (1, 1, 0), where the mode is at the top of the excitation band, the temperature-induced asymmetry is more clearly revealed [Figs. 5(e)–5(h)]. In fact, there are two broadening mechanisms of the excitation in our experiment. One is the Gaussian profile originating from the instrument resolution and mosaic spread of the sample, which is independent of temperature. The other one is the symmetric Lorentzian profile resulting from the finite lifetime of magnons, as illustrated by the dashed lines in Fig. 5. However, these two mechanisms will not give rise to the highly-asymmetric line shapes. As the scans in Fig. 5 are at relatively small $\boldsymbol{Q}$s with $H = 1$ rlu, and $K = 0.5$ and 1 rlu, phonon contributions are not significant (for $H = 1$ rlu, phonon contributions only become noticeable for $K > 3$ rlu).

Furthermore, if phonons were to contribute to the scattering, the line shapes would become broad symmetrically. As for the impurity spins, they should have strong effect at low temperatures only as shown in Fig. 1(c), and will not give rise to the asymmetric line shapes, which are only significant at high temperatures either. Therefore, the asymmetric line shapes must be an intrinsic property of $Na_2Cu_2TeO_6$ related to the Cu spins. As in previous studies [37,38,41,42], to account for the asymmetry, we use a function consisting of a modified Lorentzian convoluted with a Gaussian function, which represents the instrument resolution, to fit our data:

$$I(\boldsymbol{Q},E) = A(\boldsymbol{Q}) \int_{-\infty}^{\infty} dt \frac{\exp\left\{-\frac{[E-\Gamma(\boldsymbol{Q})t-E_0(\boldsymbol{Q})]^2}{2\sigma^2(E)}\right\}}{\sqrt{2\pi\sigma^2(E)}} \times \left\{\frac{1}{\pi}\frac{1}{1+[t-\alpha(\boldsymbol{Q})t^2+\beta(\boldsymbol{Q})t^3]^2}+c_0\right\}. \quad (3)$$

Here, $A(\boldsymbol{Q})$ is the overall amplitude, $t$ represents $[E' - E_0(\boldsymbol{Q})]/\Gamma(\boldsymbol{Q})$ [$\Gamma(\boldsymbol{Q})$ is the half width at half maximum of the Lorentzian function], $E_0(\boldsymbol{Q})$ is the center of the peak, and $\sigma$ is the variance of the Guassian indicative of the instrument resolution. $\beta(\boldsymbol{Q})$ is the damping term and $c_0$ is a constant. The

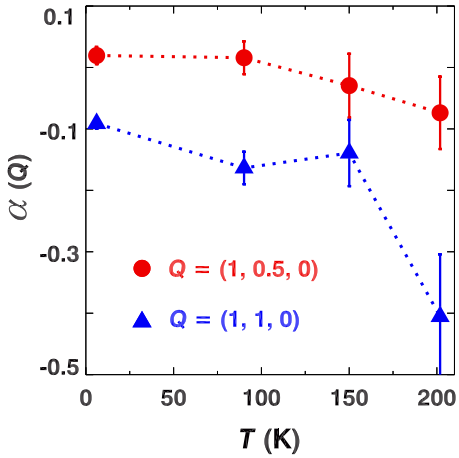


FIG. 6. Temperature dependence of the asymmetry factor $\alpha(\boldsymbol{Q})$ extracted from fits with Eq. (3) to the data in Fig. 5.

asymmetry is controlled by $\alpha(\boldsymbol{Q})$, and the sign of $\alpha(\boldsymbol{Q})$ governs whether the peak broadens to higher [$\alpha(\boldsymbol{Q}) > 0$] or lower energies [$\alpha(\boldsymbol{Q}) < 0$]. When $\alpha(\boldsymbol{Q})$, $\beta(\boldsymbol{Q}) = 0$, the modified Lorentzian profile becomes a regular symmetric Lorentzian. The data can be fitted reasonably well with Eq. (3) as shown in Fig. 5. In fact, we have also tried to fit the data with the modified Lorentzian function only without convoluting the resolution (not shown) and compared the fitting curves and output parameters by the two approaches. We find that there is no much difference between them except that the instrument resolution has a marginal effect on the broadening of the line shape. We extract the temperature dependence of the asymmetry indicator $\alpha(\boldsymbol{Q})$, and plot it in Fig. 6. The value of $\alpha(\boldsymbol{Q})$ is much larger at (1, 1, 0) than that at (1, 0.5, 0), indicating a much larger asymmetry of the line shape as can be visualized from Fig. 5. At both $\boldsymbol{Q}$s, $\alpha(\boldsymbol{Q})$ increases with temperature, which is in excellent agreement with the more pronounced asymmetric Lorentzian-type line shape in Fig. 5. At high temperatures, the asymmetry parameter at (1, 0.5, 0) and (1, 1, 0) are both negative, indicating that the peak broadens to lower energies.

## IV. DISCUSSIONS

Our INS results on the spin dynamics of $Na_2Cu_2TeO_6$ characterize it as an alternating AFM-FM chain compound with a weak but finite interchain coupling and a limited phase space due to the large $\Delta/B$. Notably, by mapping the magnetic spectra at elevated temperatures combined with the constant-$\boldsymbol{Q}$ cuts, we find that the available phase space for the triplons is more limited at high temperatures. Meanwhile, we observe an asymmetric Lorentzian-type energy broadening, which gets more pronounced as the temperature is raised shown in Fig. 5. Furthermore, we quantitatively parametrize the temperature evolution of the asymmetric energy broadening by fitting the constant-$\boldsymbol{Q}$ cuts to an asymmetric Lorentzian function convoluted with the instrument resolution. The asymmetric parameter $\alpha(\boldsymbol{Q})$ increases with increasing temperature. Our results on the asymmetric Lorentzian-type energy broadenings reflect the intrinsic properties of the Cu spins and are compelling evidence for the strong correlations at finite temperatures in $Na_2Cu_2TeO_6$ (Refs. [37–45]). Considering the weak two-dimensionality of the magnetic interactions and the alternating antiferromagnetic-ferromagnetic couplings along the chain in $Na_2Cu_2TeO_6$, our results indicate the universal presence of strongly correlated states in a broad range of quantum systems, beyond spin chains [37,40–43], spin ladders [44,45], as well as three-dimensional quantum magnets [38,39].

We believe the microscopic origin of the asymmetric line shape and the strong correlation state at finite temperatures is the hard-core constraint and small available phase space for quasiparticle scattering [33–41]. For dimerized magnets, the excitations are spin-1 triplons created by exciting a dimer from a singlet to a triplet. These quasiparticles are subject to hard-core constraint, with which they cannot occupy the same dimer site. At finite temperatures, a significant number of dimer triplets are thermally activated. In the case that the available space is limited with quasi-one-dimensionality and large $\Delta/B$, the neutron-excited triplons will interact strongly with the nearby thermally-activated triplons due to the hard-core constraint. The combined effect of a smaller phase space and larger thermal population of triplons with increasing temperature will give rise to a more asymmetric line shape as described in the text for $Na_2Cu_2TeO_6$ due to the hard-core constraint, as is also the case for other dimerized systems [37–45]. We notice that the asymmetry has a strong $\boldsymbol{Q}$-dependence, which should be related to the interaction strength and the density of states of the triplons [38,41]. Because of the strong correlation effect at high temperatures, random phase approximation calculations may not describe the high-temperature data well as they ignore correlations between the triplons [23,30,37,38,42].

## V. CONCLUSIONS

Our comprehensive INS excitation spectra clearly identify $Na_2Cu_2TeO_6$ to be an alternating AFM-FM chain compound with weak but nonzero interchain coupling. More importantly, we find the energy scans show asymmetric line shapes at elevated temperatures different from conventional magnets. The asymmetry becomes more pronounced accompanying the reduced phase space for the triplons and the increasing population of temperature-activated triplons as the temperature is raised. We take it as compelling evidence that in a weakly two-dimensional alternating AFM-FM dimer magnet $Na_2Cu_2TeO_6$, the triplons, which are subject to the hard-core constraint interact more strongly at high temperatures. These results indicate the presence of strongly correlated state in a broad range of quantum magnetic systems. Such systems with the capability of countering thermal decoherence may find future applications in quantum information and computation [53,54].

## ACKNOWLEDGMENTS

We would like to thank Rui Chen and Prof. Junfeng Wang at Wuhan National High Magnetic Field Center for assisting us in measuring the magnetization under high magnetic fields. The work was supported by National Key Projects for Research and Development of China with Grant No. 2021YFA1400400, National Natural Science Foundation of

China with Grant Nos. 11822405, 12074174, 12074175, 11774152, 11904170, and 12004191, Natural Science Foundation of Jiangsu province with Grant Nos. BK20180006, BK20190436, and BK20200738, Hubei Provincial Natural Science Foundation of China with Grant No. 2021CFB238, Fundamental Research Funds for the Central Universities with Grant No. 020414380183, and the Office of International Cooperation and Exchanges of Nanjing University. We acknowledge the neutron beam time from ISIS with Proposal No. 2010131 and from J-PARC with Proposal No. 2020A0037. Z.M. thanks Beijing National Laboratory for Condensed Matter Physics for funding support.

[1] I. Affleck, Quantum spin chains and the Haldane gap, J. Phys.: Condens. Matter **1**, 3047 (1989).

[2] B. Leuenberger, A. Stebler, H. U. Güdel, A. Furrer, R. Feile, and J. K. Kjems, Spin dynamics of an isotropic singlet-ground-state antiferromagnet with alternating strong and weak interactions: An inelastic-neutron-scattering study of the dimer compound $Cs_3Cr_2Br_9$, Phys. Rev. B **30**, 6300 (1984).

[3] J. P. Renard, M. Verdaguer, L. P. Regnault, W. A. C. Erkelens, J. Rossat-Mignod, J. Ribas, W. G. Stirling, and C. Vettier, Quantum energy gap in two quasi-one-dimensional $S = 1$ Heisenberg antiferromagnets, J. Appl. Phys. **63**, 3538 (1988).

[4] R. M. Morra, W. J. L. Buyers, R. L. Armstrong, and K. Hirakawa, Spin dynamics and the Haldane gap in the spin-1 quasi-one-dimensional antiferromagnet $CsNiCl_3$, Phys. Rev. B **38**, 543 (1988).

[5] K. Hida, Ground-state phase diagram of the spin-1/2 ferromagnetic-antiferromagnetic alternating Heisenberg chain with anisotropy, Phys. Rev. B **46**, 8268 (1992).

[6] L. P. Regnault, I. Zaliznyak, J. P. Renard, and C. Vettier, Inelastic-neutron-scattering study of the spin dynamics in the Haldane-gap system $Ni(C_2H_8N_2)_2NO_2ClO_4$, Phys. Rev. B **50**, 9174 (1994).

[7] A. Zheludev, S. E. Nagler, S. M. Shapiro, L. K. Chou, D. R. Talham, and M. W. Meisel, Spin dynamics in the linear-chain $S = 1$ antiferromagnet $Ni(C_3H_{10}N_2)_2N_3(ClO_4)$, Phys. Rev. B **53**, 15004 (1996).

[8] G. S. Uhrig and H. J. Schulz, Magnetic excitation spectrum of dimerized antiferromagnetic chains, Phys. Rev. B **54**, R9624 (1996).

[9] G. Xu, J. F. DiTusa, T. Ito, K. Oka, H. Takagi, C. Broholm, and G. Aeppli, $Y_2BaNiO_5$: A nearly ideal realization of the $S = 1$ Heisenberg chain with antiferromagnetic interactions, Phys. Rev. B **54**, R6827 (1996).

[10] N. Cavadini, G. Heigold, W. Henggeler, A. Furrer, H.-U. Güdel, K. Krämer, and H. Mutka, Magnetic excitations in the quantum spin system $TlCuCl_3$, Phys. Rev. B **63**, 172414 (2001).

[11] K. P. Schmidt and G. S. Uhrig, Excitations in One-Dimensional $S = \frac{1}{2}$ Quantum Antiferromagnets, Phys. Rev. Lett. **90**, 227204 (2003).

[12] D. A. Tennant, C. Broholm, D. H. Reich, S. E. Nagler, G. E. Granroth, T. Barnes, K. Damle, G. Xu, Y. Chen, and B. C. Sales, Neutron scattering study of two-magnon states in the quantum magnet copper nitrate, Phys. Rev. B **67**, 054414 (2003).

[13] K. P. Schmidt, C. Knetter, and G. S. Uhrig, Spectral properties of the dimerized and frustrated $S = 1/2$ chain, Phys. Rev. B **69**, 104417 (2004).

[14] E. S. Klyushina, A. T. M. N. Islam, J. T. Park, E. A. Goremychkin, E. Wheeler, B. Klemke, and B. Lake, Hamiltonian of the $S = \frac{1}{2}$ dimerized antiferromagnetic-ferromagnetic quantum spin chain $BaCu_2V_2O_8$, Phys. Rev. B **98**, 104413 (2018).

[15] H. Kageyama, M. Nishi, N. Aso, K. Onizuka, T. Yosihama, K. Nukui, K. Kodama, K. Kakurai, and Y. Ueda, Direct Evidence for the Localized Single-Triplet Excitations and the Dispersive Multitriplet Excitations in $SrCu_2(BO_3)_2$, Phys. Rev. Lett. **84**, 5876 (2000).

[16] N. Aso, H. Kageyama, K. Nukui, M. Nishi, H. Kadowaki, Y. Ueda, and K. Kakurai, High energy-resolution inelastic neutron scattering experiments on triplet bound state excitations in $SrCu_2(BO_3)_2$, J. Phys. Soc. Jpn. **74**, 2189 (2005).

[17] B. D. Gaulin, S. H. Lee, S. Haravifard, J. P. Castellan, A. J. Berlinsky, H. A. Dabkowska, Y. Qiu, and J. R. D. Copley, High-Resolution Study of Spin Excitations in the Singlet Ground State of $SrCu_2(BO_3)_2$, Phys. Rev. Lett. **93**, 267202 (2004).

[18] J. Romhányi, K. Penc, and R. Ganesh, Hall effect of triplons in a dimerized quantum magnet, Nat. Commun. **6**, 6805 (2015).

[19] K. W. Plumb, K. Hwang, Y. Qiu, L. W. Harriger, G. E Granroth, A. I Kolesnikov, G. J. Shu, F. C. Chou, C. Rüegg, Y. B. Kim, and Y.-J. Kim, Quasiparticle-continuum level repulsion in a quantum magnet, Nat. Phys. **12**, 224 (2015).

[20] P. A. McClarty, F. Krüger, T. Guidi, S. F. Parker, K. Refson, A. W. Parker, D. Prabhakaran, and R. Coldea, Topological triplon modes and bound states in a Shastry-Sutherland magnet, Nat. Phys. **13**, 736 (2017).

[21] K. Nawa, K. Tanaka, N. Kurita, T. J. Sato, H. Sugiyama, H. Uekusa, S. Ohira-Kawamura, K. Nakajima, and H. Tanaka, Triplon band splitting and topologically protected edge states in the dimerized antiferromagnet, Nat. Commun. **10**, 2096 (2019).

[22] T. Barnes, J. Riera, and D. A. Tennant, $S = \frac{1}{2}$ alternating chain using multiprecision methods, Phys. Rev. B **59**, 11384 (1999).

[23] G. Xu, C. Broholm, D. H. Reich, and M. A. Adams, Triplet Waves in a Quantum Spin Liquid, Phys. Rev. Lett. **84**, 4465 (2000).

[24] J. Xu, A. Assoud, N. Soheilnia, S. Derakhshan, H. L. Cuthbert, J. E. Greedan, M. H. Whangbo, and H. Kleinke, Synthesis, structure, and magnetic properties of the layered copper (II) oxide $Na_2Cu_2TeO_6$, Inorg. Chem. **44**, 5042 (2005).

[25] K. Morimoto, Y. Itoh, K. Yoshimura, M. Kato, and K. Hirota, Hole doping effects on spin-gapped $Na_2Cu_2TeO_6$ via topochemical Na deficiency, J. Phys. Soc. Jpn. **75**, 083709 (2006).

[26] S. Derakhshan, H. L. Cuthbert, J. E. Greedan, B. Rahaman, and T. Saha-Dasgupta, Electronic structures and low-dimensional magnetic properties of the ordered rocksalt oxides $Na_3Cu_2SbO_6$ and $Na_2Cu_2TeO_6$, Phys. Rev. B **76**, 104403 (2007).

[27] H.-J. Koo and M.-H. Whangbo, Analysis of the spin lattice model for the spin-gapped layered compounds $Na_3Cu_2SbO_6$

and $Na_2Cu_2TeO_6$ on the basis of electronic structure calculations, Inorg. Chem. **47**, 128 (2008).

[28] M. Schmitt, O. Janson, S. Golbs, M. Schmidt, W. Schnelle, J. Richter, and H. Rosner, Microscopic magnetic modeling for the $S = \frac{1}{2}$ alternating-chain compounds $Na_3Cu_2SbO_6$ and $Na_2Cu_2TeO_6$, Phys. Rev. B **89**, 174403 (2014).

[29] R. Sankar, I. Panneer Muthuselvam, G. J. Shu, W. T. Chen, S. K. Karna, R. Jayavel, and F. C. Chou, Crystal growth and magnetic ordering of $Na_2Ni_2TeO_6$ with honeycomb layers and $Na_2Cu_2TeO_6$ with Cu spin dimers, Cryst. Eng. Commun. **16**, 10791 (2014).

[30] S. Gao, L.-F. Lin, A. F. May, B. K. Rai, Q. Zhang, E. Dagotto, A. D. Christianson, and M. B. Stone, Weakly coupled alternating $S = \frac{1}{2}$ chains in the distorted honeycomb lattice compound $Na_2Cu_2TeO_6$, Phys. Rev. B **102**, 220402(R) (2020).

[31] Y. Miura, R. Hirai, Y. Kobayashi, and M. Sato, Spin-gap behavior of $Na_3Cu_2SbO_6$ with distorted honeycomb structure, J. Phys. Soc. Jpn. **75**, 084707 (2006).

[32] Y. Miura, Y. Yasui, T. Moyoshi, M. Sato, and K. Kakurai, Magnetic excitations of spin-gap system $Na_3Cu_2SbO_6$ with distorted honeycomb structure, J. Phys. Soc. Jpn. **77**, 104709 (2008).

[33] A. J. A. James, F. H. L. Essler, and R. M. Konik, Finite-temperature dynamical structure factor of alternating Heisenberg chains, Phys. Rev. B **78**, 094411 (2008).

[34] F. H. L. Essler and R. M. Konik, Finite-temperature lineshapes in gapped quantum spin chains, Phys. Rev. B **78**, 100403(R) (2008).

[35] F. H. L. Essler and R. M. Konik, Finite-temperature dynamical correlations in massive integrable quantum field theories, J. Stat. Mech. (2009) P09018.

[36] W. D. Goetze, U. Karahasanovic, and F. H. L. Essler, Low-temperature dynamical structure factor of the two-leg spin-$\frac{1}{2}$ Heisenberg ladder, Phys. Rev. B **82**, 104417 (2010).

[37] D. A. Tennant, B. Lake, A. J. A. James, F. H. L. Essler, S. Notbohm, H.-J. Mikeska, J. Fielden, P. Kögerler, P. C. Canfield, and M. T. F. Telling, Anomalous dynamical line shapes in a quantum magnet at finite temperature, Phys. Rev. B **85**, 014402 (2012).

[38] D. L. Quintero-Castro, B. Lake, A. T. M. N. Islam, E. M. Wheeler, C. Balz, M. Månsson, K. C. Rule, S. Gvasaliya, and A. Zheludev, Asymmetric Thermal Line Shape Broadening in a Gapped 3D Antiferromagnet: Evidence for Strong Correlations at Finite Temperature, Phys. Rev. Lett. **109**, 127206 (2012).

[39] J. Jensen, D. L. Quintero-Castro, A. T. M. N. Islam, K. C. Rule, M. Månsson, and B. Lake, Lineshape of the singlet-triplet excitations in the dimer system $Sr_3Cr_2O_8$ to first order in the high-density $1/z$ expansion, Phys. Rev. B **89**, 134407 (2014).

[40] B. Fauseweh, J. Stolze, and G. S. Uhrig, Finite-temperature line shapes of hard-core bosons in quantum magnets: A diagrammatic approach tested in one dimension, Phys. Rev. B **90**, 024428 (2014).

[41] E. S. Klyushina, A. C. Tiegel, B. Fauseweh, A. T. M. N. Islam, J. T. Park, B. Klemke, A. Honecker, G. S. Uhrig, S. R. Manmana, and B. Lake, Magnetic excitations in the $S = \frac{1}{2}$ antiferromagnetic-ferromagnetic chain compound $BaCu_2V_2O_8$ at zero and finite temperature, Phys. Rev. B **93**, 241109(R) (2016).

[42] F. Groitl, T. Keller, K. Rolfs, D. A. Tennant, and K. Habicht, Anomalous thermal decoherence in a quantum magnet measured with neutron spin echo spectroscopy, Phys. Rev. B **93**, 134404 (2016).

[43] E. Coira, P. Barmettler, T. Giamarchi, and C. Kollath, Finite-temperature dynamical correlations for the dimerized spin-$\frac{1}{2}$ chain, Phys. Rev. B **98**, 104435 (2018).

[44] T. Masuda, A. Zheludev, H. Manaka, L.-P. Regnault, J.-H. Chung, and Y. Qiu, Dynamics of Composite Haldane Spin Chains in IPA$-CuCl_3$, Phys. Rev. Lett. **96**, 047210 (2006).

[45] A. Zheludev, V. O. Garlea, L.-P. Regnault, H. Manaka, A. Tsvelik, and J.-H. Chung, Extended Universal Finite-$T$ Renormalization of Excitations in a Class of One-Dimensional Quantum Magnets, Phys. Rev. Lett. **100**, 157204 (2008).

[46] R. I. Bewley, T. Guidi, and S. Bennington, MERLIN: A high count rate chopper spectrometer at ISIS, Notiz. Neutr. Luce Sincro. **14**, 22 (2009).

[47] R. Kajimoto, M. Nakamura, Y. Inamura, F. Mizuno, K. Nakajima, S. Ohira-Kawamura, T. Yokoo, T. Nakatani, R. Maruyama, K. Soyama *et al.*, The Fermi chopper spectrometer 4SEASONS at J-PARC, J. Phys. Soc. Jpn. **80**, SB025 (2011).

[48] R. A. Ewings, A. Buts, M. D. Le, J. van Duijn, I. Bustinduy, and T. G. Perring, Horace: Software for the analysis of data from single crystal spectroscopy experiments at time-of-flight neutron instruments, Nucl. Instrum. Methods Phys. Res., Sect. A **834**, 132 (2016).

[49] J. W. Hall, W. E. Marsh, R. Weller, and W. Hatfield, Exchange coupling in the alternating chain compounds catena-di-micron-chlorobis(4-methylpyridine)copper(II), catena-di-micron-bromobis-(N-methylimidazole)copper(II), catena-hexanedionebis(thiosemicarbazato)copper(II), and catena-octanedionebis(thiosemicarbazato)copper(II). Inorg. Chem. **20**, 1033 (1981).

[50] J. J. Borrás-Almenar, E. Coronado, J. Curély, R. Georges, and J. Gianduzzo, Alternating Chains with Ferromagnetic and Antiferromagnetic Interactions. Theory and Magnetic Properties.

[51] M. P. Nightingale and H. W. J. Blöte, Gap of the linear spin-1 Heisenberg antiferromagnet: A Monte Carlo calculation, Phys. Rev. B **33**, 659 (1986).

[52] T. Jolicoeur and O. Golinelli, $\sigma$-model study of Haldane-gap antiferromagnets, Phys. Rev. B **50**, 9265 (1994).

[53] L. Amico, R. Fazio, A. Osterloh, and V. Vedral, Entanglement in many-body systems, Rev. Mod. Phys. **80**, 517 (2008).

[54] M. A Nielsen and I. Chuang, *Quantum Computation and Quantum Information* (Cambridge University Press, Cambridge, 2010).